ALEPH 86-46
W. Witzeling
8.4.1986 Distr.: TPC

EUROPEAN ORGANIZATION FOR NUCLEAR RESEARCH

TPC90, a Test Model for the ALEPH Time Projection Chamber

S.R.Amendolia[6], R.Benetta[1], M.Binder[8], W.Blum[5], A.Caldwell[8], M.Cherney[8], D.F.Cowen[8], D.DeMille[8], A.Farilla[1], F.Fidecaro[6], Y.N.Guo[8], J.M.Izen[8], R.C.Jared[8], W.Kilgore[8], K.Kleinknecht[2], I.Lehraus[1], F.Liello[7], J.J.Love[8], A.Lusiani[6], P.Maas[8], P.S.Marrocchesi[6], R.Matthewson[1], J.May[1], M.Mermikides[8], E.Milotti[7], A.Minten[1], E.Monnier[1], D.Muller[8], A.Peisert[5], M.J.Price[1], F.Ragusa[7], C.Raine[3], J.Richstein[2], R.Richter[5], L.Rolandi[7], G.Sanguinetti[1], W.D.Schlatter[1], J.Sedgebeer[4], R.Settles[5], G.Sinnis[8], K.M.Smith[3], G.Stefanini[1], U.Stierlin[5], M.Takashima[8], W.Tejessy[1], J.Thomas[1], A.Vayaki[1], J.Wells[3], E.Wicklund[8], W.Witzeling[1], S.L.Wu[8], W.M.Wu[1]
(presented by W.Witzeling)

[1] CERN European Organisation for Nuclear Research, Geneva, Switzerland
[2] Institut f. Exp. Physik IV, University of Dortmund, Dortmund, FRG
[3] Department of Natural Philosophy, University of Glasgow, UK
[4] Department of Physics, Imperial College, London, UK
[5] Max Planck Institut f. Physik and Astrophysik, Munich, FRG
[6] Dipartimento di Fisica, Sezione INFN and Scuola Normale, Pisa, Italy
[7] Dipartimento di Fisica and Sezione INFN, Trieste, Italy
[8] Department of Physics, University of Wisconsin, Madison, Wisc., USA

Geneva, 26 February, 1986

Abstract: A test model has been built to study the performance of prototypes for the ALEPH Time Projection Chamber. The device consists of a solenoid magnet providing a magnetic field of up to 1.2 Tesla inside a cylindric field cage of 75 cm diameter and 1.3 m length. It has been used to test two chambers of different design. We describe the setup and present results from measurements with these prototype chambers using laser beams and cosmic ray particles.

1. Introduction

The ALEPH collaboration is currently preparing an experiment [1] at the new Large Electron Positron collider (LEP) which is now under construction at CERN. For the central detector the ALEPH collaboration has decided to build a large time projection chamber (TPC) based on the pioneering work of D.Nygren et al. [2] provided that a system of laser rays can be incorporated for the calibration of the large drift volume and that the build-up of space charge can be avoided by gating the TPC. Therefore TPC90 was built as a testing facility to study the performance of prototype chambers under realistic conditions (i.e. with long drift distance in magnetic field), to test laser beams, to study systematic effects (influence of field inhomogeneities, diffusion, gas parameters etc) and to test the gating concept. Furthermore it should serve as a testing ground for new electronics and a new readout system which is being developed for the ALEPH TPC and last but not least to gain operational experience with such detectors.

2. TPC90

A cutoff view of the set up is shown in fig. 1. It consists of a solenoid magnet with an iron return yoke providing a magnetic field in a cylindrical volume, in which is inserted a field cage producing an electric field parallel to the magnetic field. The field cage is closed on one side by a high voltage electrode which for special studies has a central quartz window of 150 mm diameter. On the opposite side the drift volume is closed by the TPC endplate, a MWPC chamber with segmented cathode read-out. Tracks are produced inside the drift volume by laser rays passing through windows or by cosmic particles traversing the detector. In the following the different components of the setup are described.

2.1 The Magnet

The magnet is a watercooled 175 cm long solenoid with inner diameter 90 cm which is enclosed by two iron end plates and 20 iron slabs forming the return yoke. The coil is made out of 68 pancakes and contains three gaps to allow the traversal of laser rays. The pancakes were designed such to op-

timize the azimuthal field uniformity. Electrically the coil is split into two groups of pancakes connected in parallel. Within a group the pancakes (odd or even numbered ones) are connected in series. The magnet can be operated in direct current mode up to 1820 Ampere producing a field of 7 kGauss and in pulsed mode (a typical cycle time is 12 sec with 3 sec flat top) up to 3120 Ampere corresponding to a field of 12 kGauss with a peak power consumption of 1.6 Megawatt.

2.2 The Field Cage

The field cage consists of a 10 mm thick fiberglass epoxy cylinder of 166 cm length and 75 cm inner diameter. On its inner surface are imbedded 66 copper electrode rings 2 mm thick, 19 mm wide and spaced by 1.5 mm. These rings are cut once on the circumference to avoid closed loops for eddy currents during pulsed operation of the magnet. The outer surface of the cylinder is covered with a conductive paint. The electrodes are connected to a precision resistor chain (65 x 3 MΩ) mounted on the outside of the cylinder. In the field cage imbedded are 20 quartz windows, 12 of them are oval (12 x 50 mm^2) and located at the gaps in the coil of the magnet, thus allowing laser rays to traverse the volume from outside the magnet. The field cage has been operated with high voltage up to 35 kVolt corresponding to an electric field of 260 Volt/cm.

2.3 The Gas System

The drift volume (approx. 0.6 m^3) is filled with the detector gas at atmospheric pressure. In standard operation premixed gas (Argon + 9% CH_4) is used in flow through mode. The gas system has provisions to protect the detector against under/overpressure, includes gas leak detectors, an oxygen meter[1] and a monitor chamber with a drift length of 20 cm to measure parameters directly related to the gas like gas amplification, electron attachment and drift velocity. For special studies the system is equipped with a recirculation and purification loop using an Oxisorb filter and a molecular sieve. Under normal conditions (flow rate: 80 liters/hour, no purification) the oxygen contamination is around 20 ppm. The monitor chamber

---

[1] Teledyne Model 316

has been used for many studies, one of the results concerning the signal attenuation by electron attachment is shown in fig. 2. From the slope of the measured points it can be estimated that in the case of the ALEPH TPC (i.e. for a drift length of 2.2 m) a contamination of 10 to 20 ppm of oxygen would cause an attenuation of the signal by about 1%.

2.4 The Laser System

UV lasers are convenient tools to produce straight tracks of ionisation in the presence of a magnetic field. TPC90 has two laser systems available. For most of the studies a two stage nitrogen laser[2] is used, emitting at λ = 337 nm with a pulse energy of 200 μJ and a pulse duration of 0.5 nsec. The laser ray can be brought into the detector volume through the gaps in the coil and the corresponding windows in the field cage or by means of a beam splitter system located in the gap between the coil and the field cage which produces two parallel tracks at the beginning and the end of the drift region and a 45° track.

The second laser available is a Nd-YAG laser[3] which is the type forseen for the laser calibration system of the ALEPH TPC. This laser contains a frequency quadrupler to produce light at a wavelength of λ = 266 nm with a power of 4 mJ per pulse and a pulse duration of 8 nsec and is normally used with a beam splitting system producing three parallel tracks.

2.5 The TPC90 Chambers

For the test setup two different chambers have been built. The first one was constructed in the spirit of gaining experience and is modeled after the Berkeley design [2] for PEP4. This chamber has hexagonal shape (originally considered for the elements of the ALEPH TPC) and the basic structure is made of a copper cladded fiberglass plate reinforced on the backside by a frame and stiffening ribs. The cathode plane contains 8 straight rows of pads (pad size 8 x 8 mm^2) spaced by 72 mm, which are obtained by milling

---

[2] MOPA-400, Multilasers, Geneva, Switzerland

[3] Spectron Laser Systems Ltd, Rugby, UK

away the copper. Above the cathode there are three planes of wires arranged as shown in fig. 3. The first one contains the sense and field shaping wires, the second layer forms the ground grid terminating the drift field and the third acts as the gating grid [3]. All wires are glued at the edges with Araldite to 5 mm wide frames which also contain the printed circuits for the electrical connections; the second and third wire plane are glued to removable frames. The sense wires and the pads are connected to preamplifiers located on the chamber. For the first chamber we have used 256 electronics channels identical to those of the PEP4 TPC [4].

The second chamber can be considered as a prototype for the sectors forming the endplate of the ALEPH TPC. Although not quite the size of a final sector it has all the relevant design features. The construction is based on an Aluminium sandwich, is wedge shaped and the cathode plane has long radial pads (6.7 x 30 mm^2) along concentric arcs (see fig. 4). The arrangement of the wire planes is identical to that of the first prototype. First this chamber has been operated with the previously mentioned electronics, but recently it has been equipped with new electronics designed for the ALEPH TPC. It consists of preamplifiers and line drivers in hybrid technology located on the chamber and Time Projection Digitizers (TPD) which are Fastbus modules containing each 64 channels with line reciever, shaper, FlashADC and front end memories. More details on the electronics and the read out system can be found in [5].

3. Results

From the various extensive studies which have been performed with TPC90 we will present here only a few selected results, others have been published elsewhere [6] [7] [8].

3.1 Pad Response Function

One important parameter necessary for the position determination of a track is the pad response function (PRF) which describes the dependence of the signal amplitude A_i on pad i at position y_i of an avalanche at position y of

a sense wire. It has been shown [9] that the PRF can be approximated by a Gaussian function

$$A_i = A_0 . \exp[-(y-y_i)^2/2\sigma_0^2] \qquad (1)$$

The width σ_0 depends only on the geometrical properties of the chamber. However, the diffusion of the drifting electrons and the ExB effect [10] near the sense wires influence the avalanche such that the actually measured width σ_{PRF} depends on the magnetic field and the drift length. This width σ_{PRF} can be parameterized as a convolution of Gaussian distributions of the form

$$\sigma_{PRF}^2 = \sigma_0^2 + \sigma_D^2\,(B,L) + \sigma_{ExB}^2\,(B) \qquad (2)$$

where σ_D and σ_{ExB} describe the contribution to the width caused by the diffusion and the ExB effect respectively. In equation (1) A_0, y and σ_0 are three unknowns, therefore the width of the Gaussian can be calculated for each event, if three neighbouring pads have signals of amplitude A_{i-1}, A_i, A_{i+1}, by the expression:

$$\sigma_{PRF}^2/\Delta^2 = [\ln(A_i^2/(A_{i-1} . A_{i+1}))]^{-1} \qquad (3)$$

where Δ is the pitch of the pads. This ratio (3) is plotted in fig. 5 as a function of the magnetic field for three different drift distances. (More details can be found in [8].) The strong decrease of the width with increasing magnetic field demonstrates one of the basic concepts of the TPC, namely that the magnetic field is not only used to measure the momentum of particles but also to reduce the transverse diffusion of the drifting electrons.

3.2 The Magnetic Field

We have measured the three components of the magnetic field inside the volume with the goal to measure the radial and the azimuthal component to the precision of 1 Gauss in the presence of a main component which is 10^4 times higher using five orthogonal hall probes and a laser to monitor their geometrical alignment. Knowing the main component of the magnetic field on a closed surface one can solve Maxwell's equations for a scalar potential

[11] and can calculate the three components of the magnetic field inside the enclosed volume (apart from a constant term). Comparing the measurement of the three components from a fine scan in the volume (about 5000 points) with the calculation using the above mentioned method, the discrepancy found was less than 1 Gauss (RMS value) for the main and the radial component and less than 2 Gauss for the azimuthal component. The absolute values for the radial and the azimuthal component are plotted in fig. 6 for a magnetic field of 12 kGauss.

From the measurement with a laser ray the quantity

$$\Delta_s = [\omega\tau/(1+\omega^2\tau^2)] \cdot \int(B_r/B_z)dz \qquad (4)$$

can be obtained. Knowing $\omega\tau$ (where ω is the cyclotron frequency and τ is the mean time between collisions of the drifting electron) the integral

$$\int(B_r/B_z)dz \qquad (5)$$

can be calculated. On the other hand, the integral (5) can be computed using the field map and we found good agreement between the measurement and computation; a detailed discussion of the results can be found in [7].

3.3 Straightness of Laser Tracks

The variance σ_y of the position y_i of a laser ray as measured with the chamber is of the order of 100 μm, hence the mean position $\langle y_i \rangle$ of the track at pad row i can be measured with an error of less than 10 μm with a few hundred laser shots. This makes the laser a well suited tool for the study of systematic effects. We performed a scan by displacing the laser parallel to the TPC end plate in steps of 1 mm over a range of 10 mm. Four of these measured tracks are shown in fig. 7 (note that lines have different vertical origin). Fitting a straight line to these points we obtain mean residuals between 22 and 27 μm. The reconstructed vertical distance between the tracks is 1.007 ±26 μm, which is consistent with our precision in the displacement of the laser ray.

3.4 Resolution with Cosmic Particles

With the first prototype chamber the spatial resolution was measured with cosmics and the results obtained are consistent with the expected resolution as measured with a small test chamber [10]. Here we present some preliminary results obtained with the second prototype chamber. Only five pad rows were equipped with electronics and the chamber was not tuned to optimum conditions. By means of scintillation counters triggers were accepted from cosmics traversing the detector within following limits: azimuthal angle $-7° < \phi < 7°$, polar angle $37° < \Theta < 90°$, and within the available drift lenght, i.e. between 0 and 130 cm. The data were taken at 12 kGauss and at a drift field of 113 V/cm with Ar + 9% CH_4. Defining the resolution as

$$\sigma_y^2 = \Sigma(y_i - y_{i,fit})^2 / F \qquad (6)$$

(where y_i is the measured coordinate at pad row i and $y_{i,fit}$ is the coordinate obtained with a parabolic fit to the points of each individual track, F is the number of degrees of freedom) and making only a loose cut on curved tracks we obtain a spatial resolution in the projection of the pad plane of σ_y = 210 µm. Using only the information from the pads the resolution in the drift direction is σ_z = 1.3 mm. However, for the above mentioned reasons these results still contain systematic errors.

3.5 Measurement of Ionisation Loss with Cosmic Particles

Only 52 sense wires were equipped with electronics yielding a mean value of 46 samples (sampling length 4 mm at 1 atmosphere). Sorting the tracks in momentum bins and calculating the truncated mean value of the 75% lowest of the pulseheight distribution, we obtain a resolution in the measurement of the ionisation loss of 27% FWHM, which can be cosidered as adequate within the limitations of the electronics available at this time and the momentum resolution of the prototype. The relative ionisation versus momentum of particles is plotted in fig. 8 showing the relativistic rise of the ionisation.

4. Conclusion

The test facility TPC90 proved to be an extremely valuable tool for testing protoype sectors for the ALEPH TPC, to investigate the application of laser rays and to study systematic effects in time projection chambers (e.g. pad response function, diffusion of drifting electrons, distortions of tracks due field inhomogeneities). It also allows to measure the spatial resolution obtainable with particles and to test new electronics.

Acknowledgements

The technical division of the Max-Planck-Institut fuer Physik und Astrophysik in Munich deserves special thanks for their dedicated work in designing and building a large part of the hardware of TPC90 and we would like to mention especially K.-H.Ackermann, E.Giesche, H.Muench, H.Schmuecker, H.Stieg, W.Tribanek and P.Weissbach, who were leaders in this effort.

References

[1] ALEPH collaboration, Technical Report 1983 (CERN/LEPC/83-2) and Status Report 1984 (CERN/LEPC/84-15).

[2] Proposal for the PEP4-TPC, SLAC PUB-5012 (1976); D.R.Nygren, PEP-198 (1975).

[3] S.R.Amendolia et al., Nucl. Instr. and Meth. A234 (1985) 47.
S.R.Amendolia et al., Nucl. Instr. and Meth. A239 (1985) 192.

[4] R.C.Jared et al., IEEE Trans. Nucl. Sc. Vol. NS-29 No 1, Feb 1982, 57 and references therein.

[5] A.Konoplyannikov et al., IEEE Trans. Nucl. Sc. Vol. NS-32, No 1, Feb 1985, 658.

[6] M.Benetta et al., IEEE Trans. Nucl. Sci. NS-32, No 1, Feb 1985, 605.

[7] S.R.Amendolia et al., Nucl. Instr. and Meth. A235 (1985) 296.

[8] S.R.Amendolia et al., submitted to Nucl. Instr. and Meth.

[9] D.L.Fancher and A.C.Schaffer, IEEE Trans. Nucl. Sci. NS-26 (1979) 150.

[10] S.R.Amendolia et al., Nucl. Instr. and Meth. 217 (1983) 317.
C.K.Hargrove et al., Nucl. Instr. and Meth. 219 (1984) 461.

[11] H.Wind, Nucl. Instr. and Meth. 84 (1970) 117.

Figure Captions

Fig. 1: Cutoff view of the TPC90 test setup

Fig. 2: Attenuation of the signal by electron attachment as a function of oxygen contamination measured in the monitor chamber of the gas system

Fig. 3: Schematic arrangement of the wire grids above the cathode plane

Fig. 4: Photograph of the second prototype chamber

Fig. 5: The dependence of the PRF on the magnetic field for three drift distances

Fig. 6: a) The radial component of the magnetic field plotted vs. the axial direction for different radii b) The angular component plotted vs. the azimuthal angle for different radii

Fig. 7: The straightness of reconstructed laser tracks (the tracks have different vertical origin and are spaced by 1 mm)

Fig. 8: Relative ionisation loss vs. momentum of particles

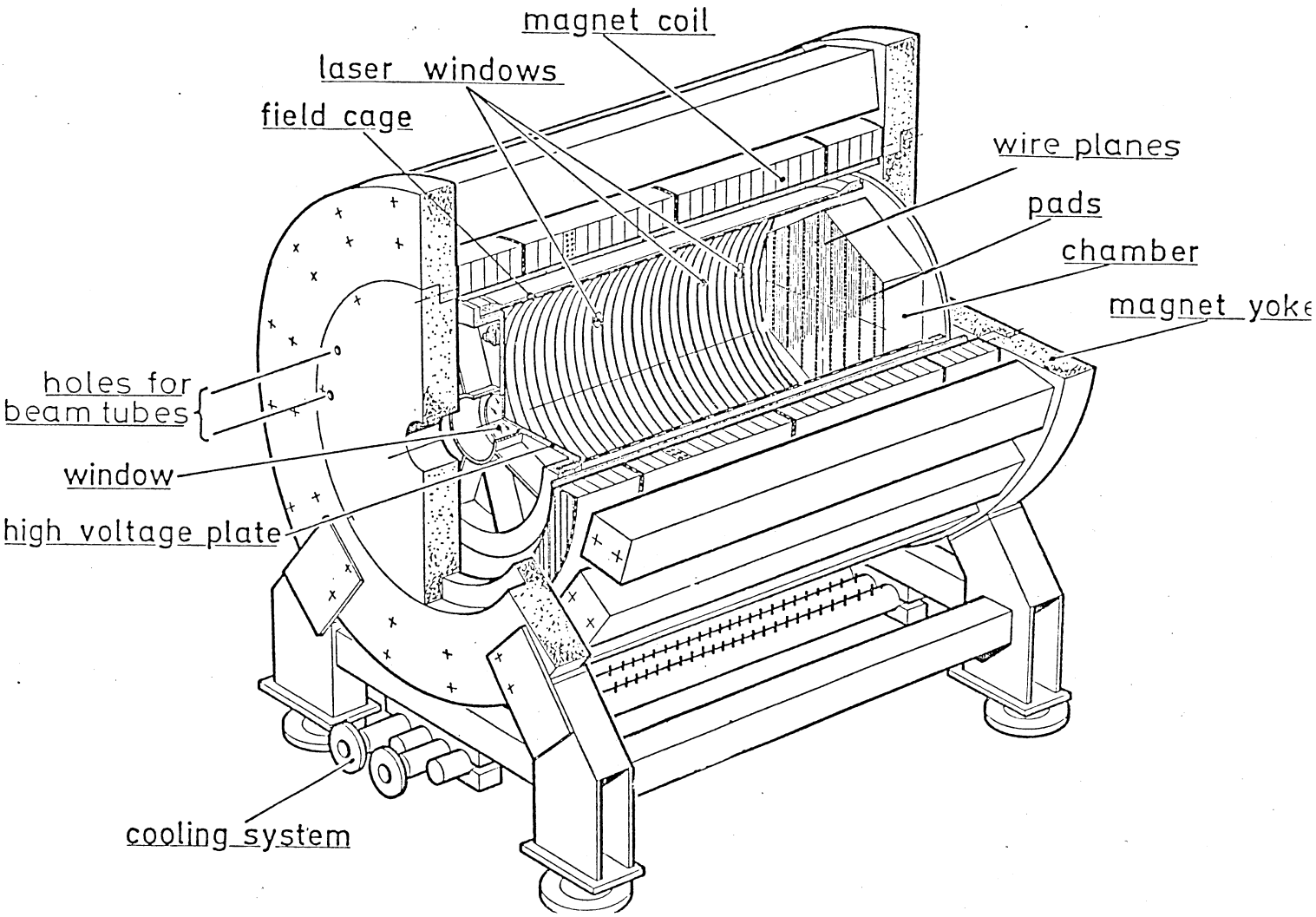
magnet coil
laser windows
field cage
wire planes
pads
chamber
magnet yoke
holes for beam tubes
window
high voltage plate
cooling system

Figure 1

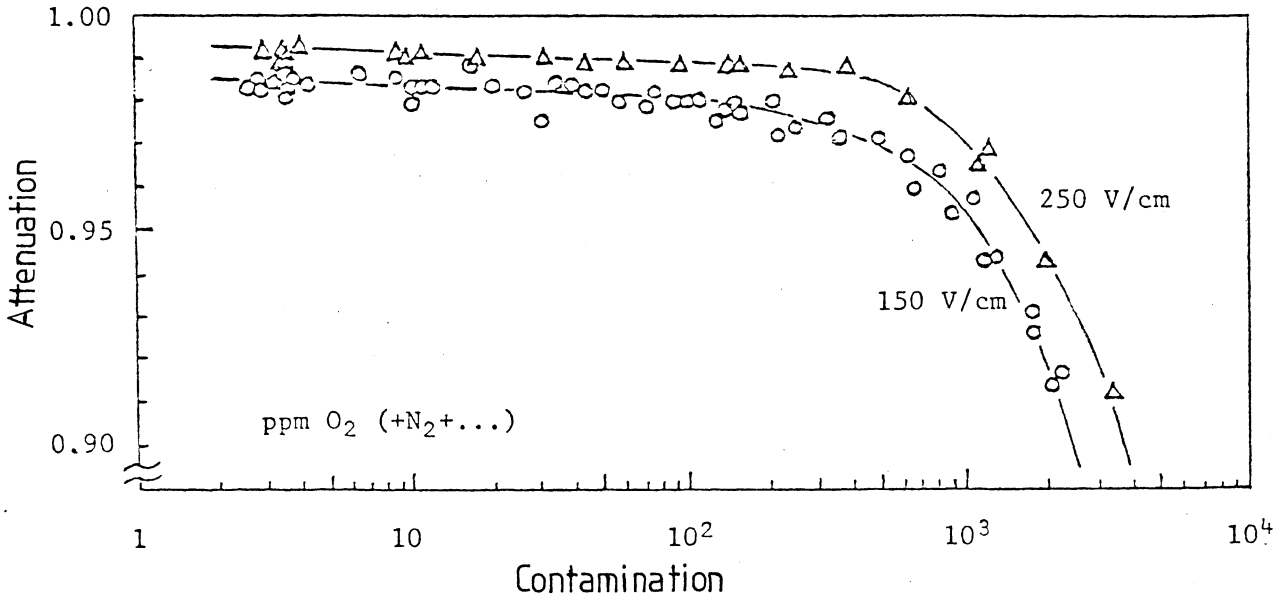
1.00
0.95
0.90
Attenuation
250 V/cm
150 V/cm
ppm O_2 (+N_2+...)
1
10
10^2
10^3
10^4
Contamination

Figure 2

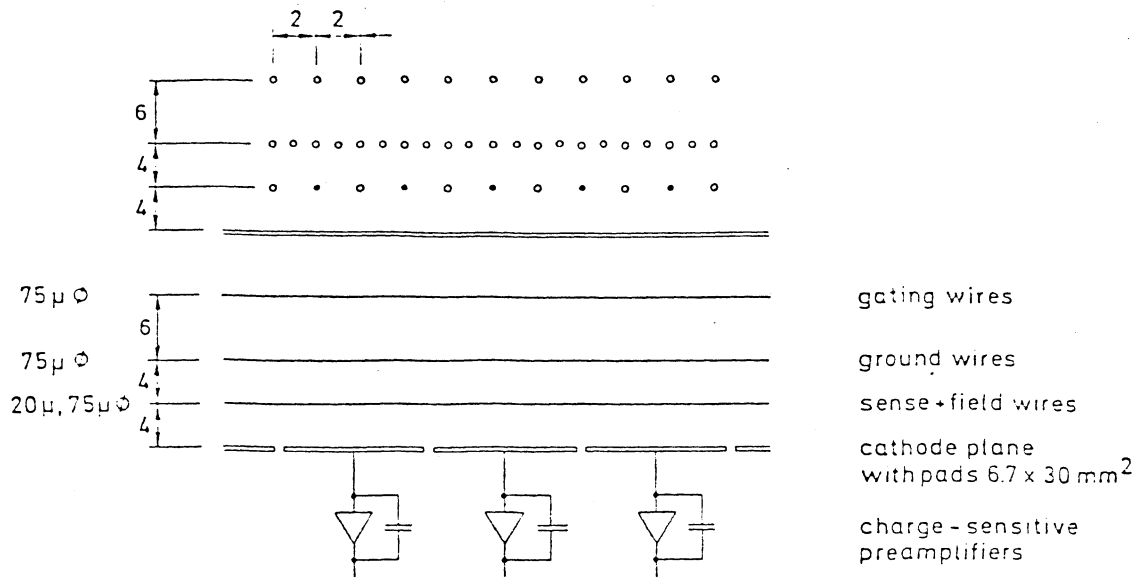
2 2
6
4
4
75 µ Ø
6
75 µ Ø
4
20 µ, 75 µ Ø
4
gating wires
ground wires
sense + field wires
cathode plane
with pads 6.7 x 30 mm²
charge - sensitive
preamplifiers

Figure 3

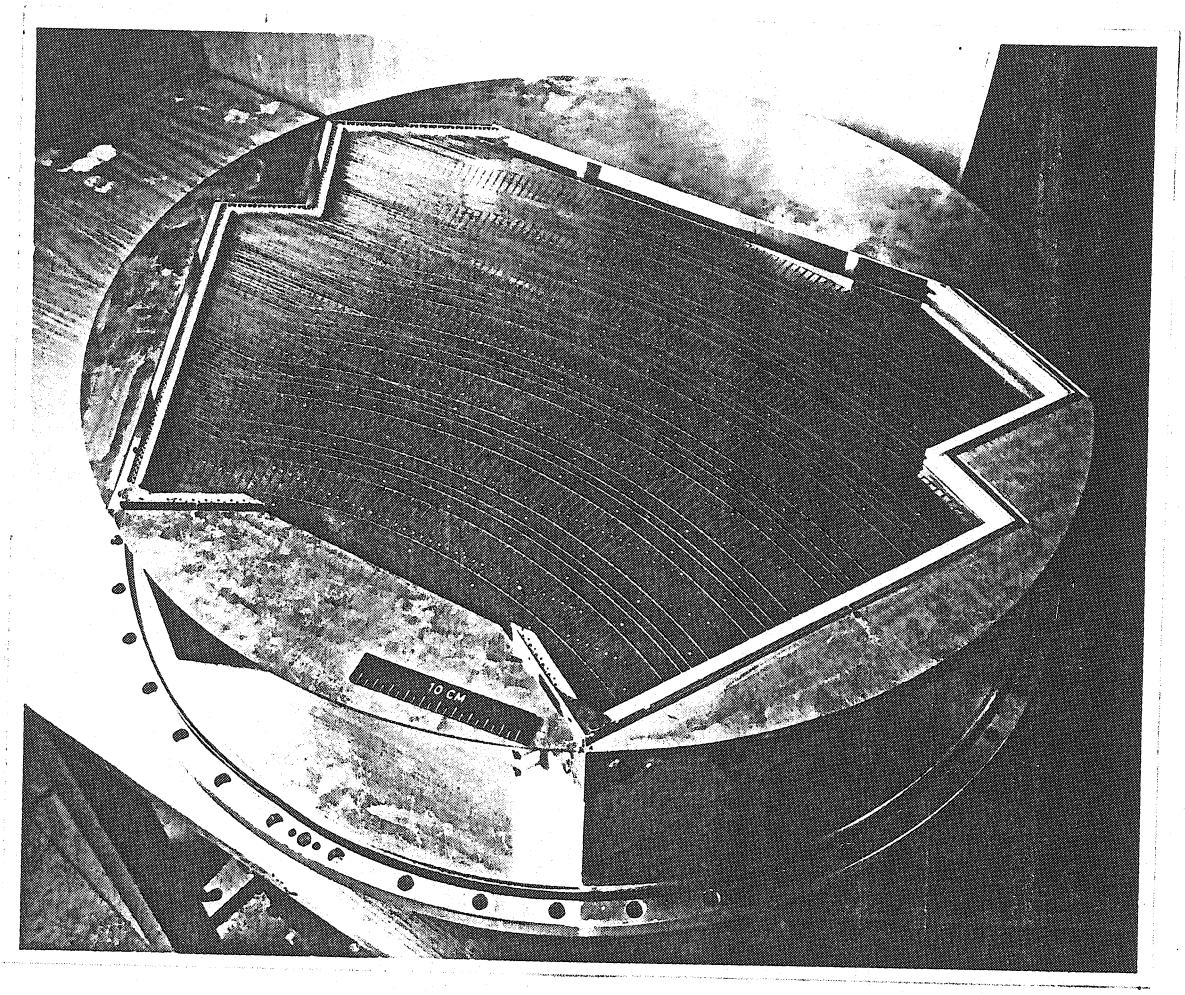

Figure 4

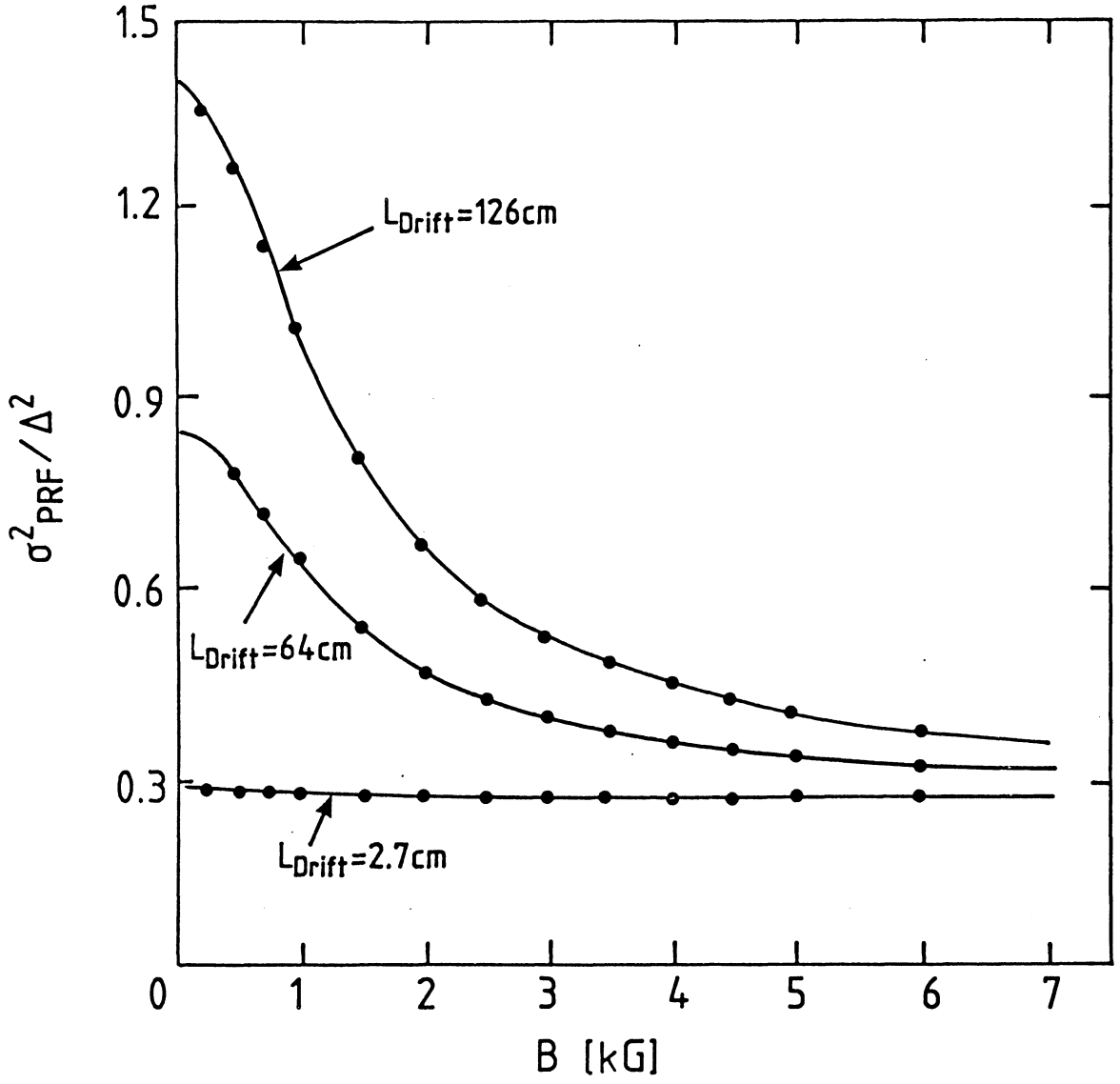
1.5
1.2
0.9
0.6
0.3
0
1
2
3
4
5
6
7
σ^2_{PRF}/Δ^2
B [kG]
L_{Drift}=126cm
L_{Drift}=64cm
L_{Drift}=2.7cm

Figure 5

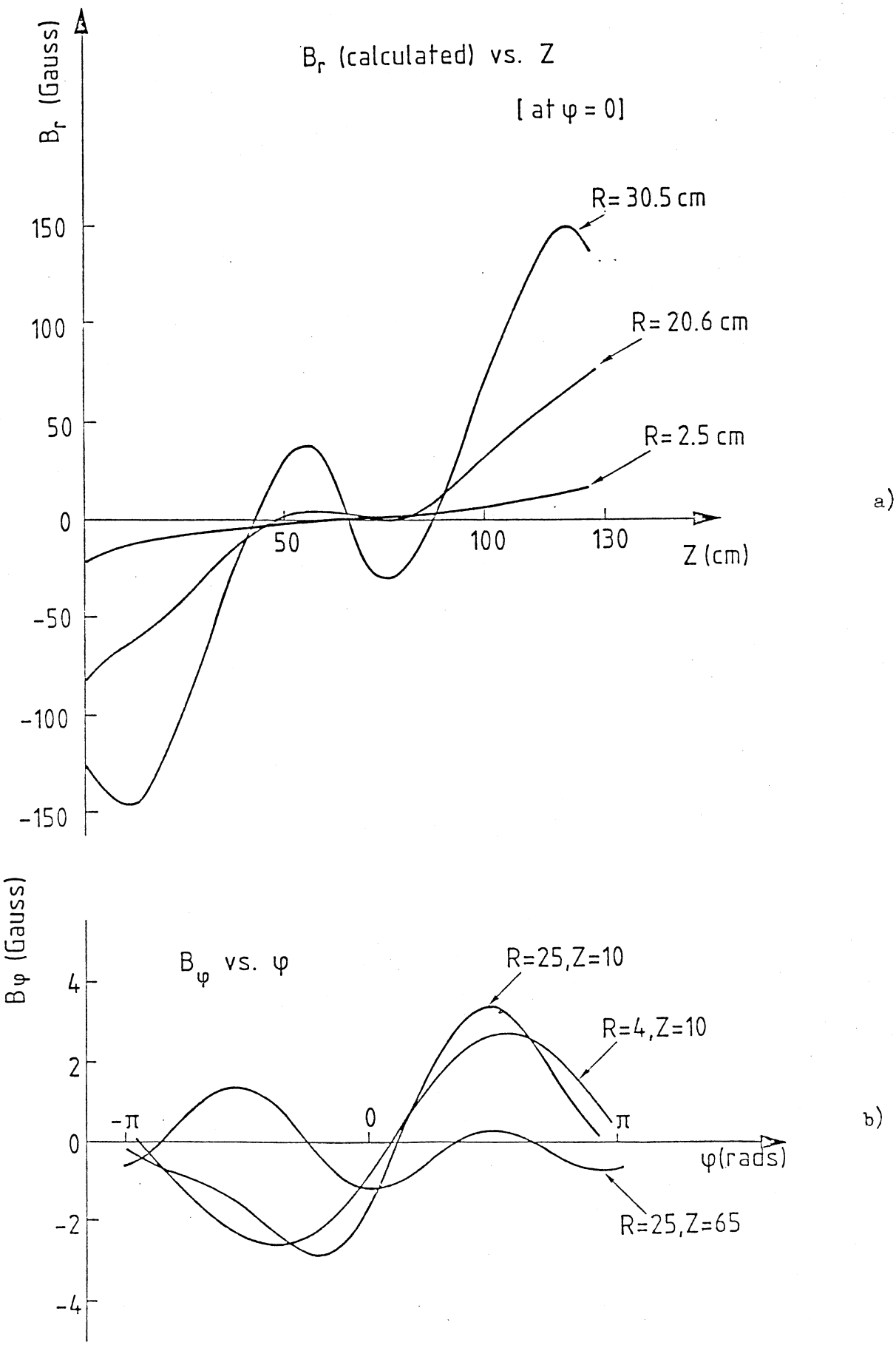
B_r (calculated) vs. Z
[at φ = 0]
B_r (Gauss)
R= 30.5 cm
R= 20.6 cm
R= 2.5 cm
150
100
50
0
-50
-100
-150
50
100
130
Z (cm)
a)
B_φ (Gauss)
B_φ vs. φ
R=25,Z=10
R=4,Z=10
R=25,Z=65
4
2
0
-2
-4
-π
0
π
φ(rads)
b)

Figure 6

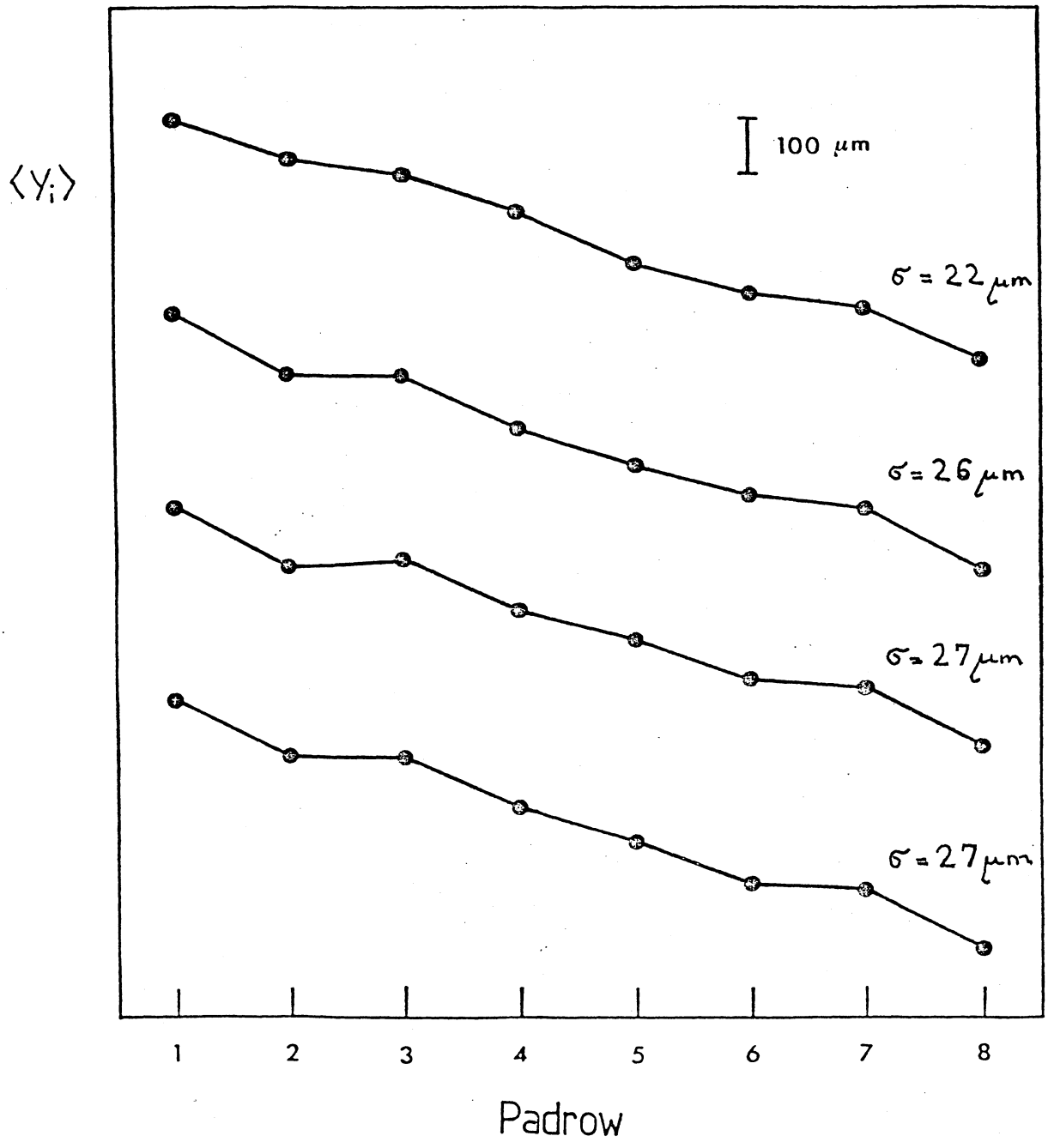

Figure 7

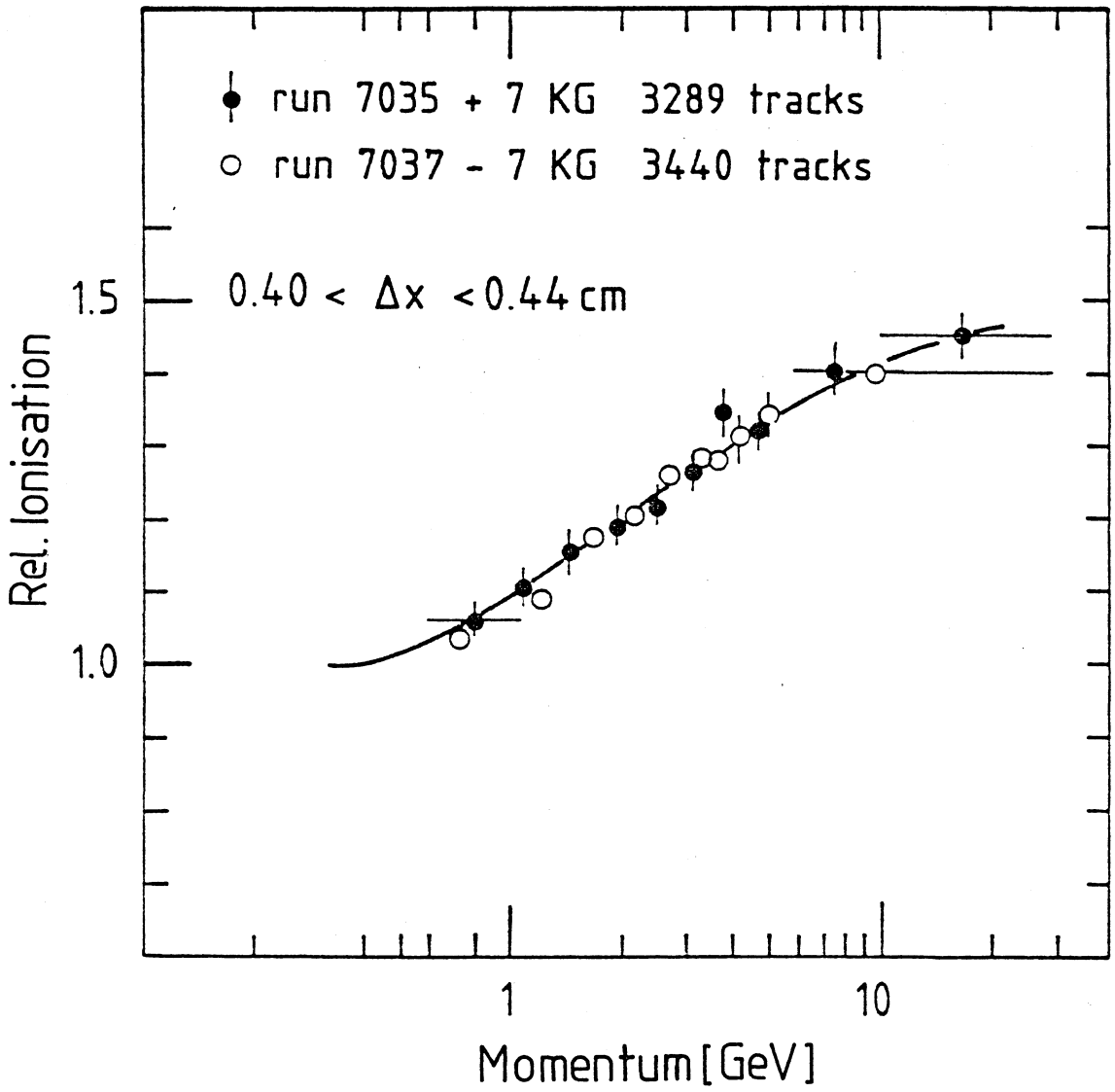
run 7035 + 7 KG 3289 tracks
run 7037 - 7 KG 3440 tracks
0.40 < Δx < 0.44 cm
Rel. Ionisation
1.5
1.0
1
10
Momentum [GeV]

Figure 8